Fluorescence Polarization of Skeletal Muscle Fibers Labeled with Rhodamine Isomers on the Myosin Heavy Chain

Christopher L. Berger,* James S. Craik,# David R. Trentham,# John E. T. Corrie,# and Yale E. Goldman*
*Department of Physiology and Pennsylvania Muscle Institute, University of Pennsylvania, Philadelphia, Pennsylvania 19104-6083 USA, and #National Institute for Medical Research, Mill Hill, London NW7 IAA, UK

ABSTRACT Fluorescence polarization was used to examine orientational changes of Rhodamine probes in single, skinned muscle fibers from rabbit psoas muscle following either photolysis of caged nucleotides or rapid length changes. Fibers were extensively and predominantly labeled at SH1 (Cys-707) of the myosin heavy chain with either the 5- or the 6-isomer of iodoacetamidotetramethylrhodamine. Results from spectroscopic experiments utilizing the two Rhodamine isomers were quite similar. Following photolysis of either caged ATP or caged ADP, probes promptly reoriented toward the muscle fiber axis. Changes in the fluorescence polarization transients elicited by the photolysis of caged ATP in the presence of saturating Ca^{2+} greatly preceded active force generation. Photolysis of caged ADP caused only a small, rapid decrease in force but elicited changes in the fluorescence polarization signals with time course and amplitude similar to those following photolysis of caged ATP. Fluorescence polarization signals were virtually unchanged by rapid length steps in both rigor and active muscle fibers. These results indicate that structural changes monitored by Rhodamine probes at SH1 are not associated directly with the force-generating event of muscle contraction. However, the fluorescence polarization transients were slightly faster than the estimated rate of cross-bridge detachment following photolysis of caged ATP, suggesting that the observed structural changes at SH1 may be involved in the communication pathway between the nucleotide- and actin-binding sites of myosin.

INTRODUCTION

At the molecular level, muscle contraction is due to the cyclic interaction of two proteins, actin and myosin, which convert the chemical energy of ATP hydrolysis into mechanical work. The conventional cross-bridge theory postulates that the myosin molecule attaches to actin and then tilts to generate force, myofilament sliding, or both (H.E. Huxley, 1969; A.F. Huxley and Simmons, 1971). Extrinsic probes attached to the catalytic domain of myosin at SH1 (Cys-707, the most reactive sulfhydryl of the myosin heavy chain) have been used in conjunction with spectroscopic techniques such as fluorescence polarization (Tregear and Mendelson, 1975; Borejdo et al., 1982), electron paramagnetic resonance (EPR; Cooke et al., 1982; Barnett and Thomas, 1989; Berger et al., 1989; Fajer et al., 1990b; Berger and Thomas, 1993), and phosphorescence anisotropy (Stein et al., 1990) to examine changes in orientation and mobility of the myosin head under a variety of conditions. However, all these previous studies lacked sufficient time resolution to correlate changes in the spectroscopic signals directly with the force-generating event of the contractile cycle.

Tanner et al. (1992), using a combination of mechanical and spectroscopic techniques with millisecond time resolution, were able to compare changes in linear dichroism from Rhodamine probes at SH1 in single rabbit psoas muscle fibers with mechanical transients elicited by photolysis of caged nucleotides (inert analogs of ATP and ADP until activated by UV light; Kaplan et al., 1978). The study of Tanner et al. found that changes in the orientation of the Rhodamine probes at SH1 accompany nucleotide binding but precede the development of force, arguing against the idea that myosin rotates as a rigid body during the power stroke. The dichroism signal used by Tanner et al. provides only one order parameter for evaluating the change in the orientational distribution of the probes at SH1 and thus cannot always distinguish between changes in average probe angle and changes in the degree of dispersion about the average angle. Furthermore, in that research the fibers were labeled by use of a commercial preparation of iodoacetamidotetramethylrhodamine (IATR) containing unknown proportions of its 5- and 6-isomers (Fig. 1). It is possible that the two isomers of Rhodamine probes, covalently bound at SH1, could adopt independent orientational distributions. Ajtai et al. (1992) reported that these isomers have different reactivities and specificity within the myofilament lattice, but their results were also obtained with probes for which no evidence of purity or isomeric ratio was presented.

Allen et al. (1996), using an improved spectroscopic technique (fluorescence polarization) capable of distinguishing changes of orientation and dispersion, studied motions of Rhodamine probes bound to the myosin regulatory light chain. Like Tanner et al. (1992), they also found orientation changes (mainly disordering) that promptly oc

Received for publication 17 June 1996 and in final form 27 August 1996.

Address reprint requests to Dr. Christopher L. Berger, Department of Molecular Physiology and Biophysics, University of Vermont College of Medicine, Burlington, VT 05405-0068 (Dr. Berger's present address). Tel.: 802-656-0832; Fax: 802-0747; E-mail: berger@salus.med.uvm.edu.

Dr. Craik's present address is Bockus Research Institute, Graduate Hospital, Philadelphia, PA 19146.

0006-3495/96/12/3330/14 $2.00

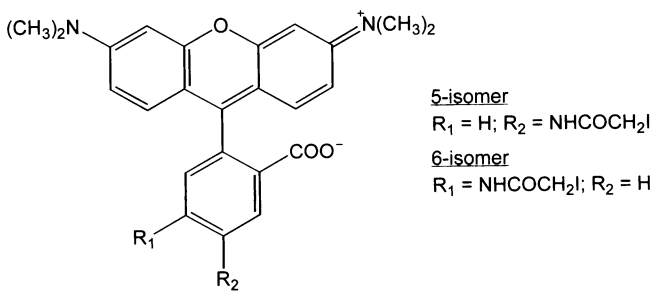

FIGURE 1 Structure of IATR.

curred following photolysis of caged ATP, with little further change in the orientation distribution during force development. Irving et al. (1995), on the other hand, detected changes in the orientation distribution of Rhodamine-labeled regulatory light chains when quick length changes were applied to isometrically contracting muscle fibers. The fluorescence polarization signals changed during the applied length changes, signaling elasticity in the cross-bridges, and also during the quick recovery of tension thought to reflect the active motions of the cross-bridges (A.F. Huxley and Simmons, 1971).

To understand the motions at the catalytic domain of myosin following photolysis of caged nucleotides and rapid length changes, we measured fluorescence polarization signals from Rhodamine probes bound to SH1 in muscle fibers. We used well-characterized, pure samples of each of the two isomers of IATR (Corrie and Craik, 1994) to eliminate possible inhomogeneity in the attachment of the probes to SH1 owing to differential reactivity or specificity of the two isomers. The present study and those of Irving et al. (1995) and Allen et al. (1996) are complementary and give dynamic structural information that distinguishes two separate locations on myosin during active force generation. Some of this research was presented previously in preliminary form (Berger et al., 1994a,b; 1995a,b).

MATERIALS AND METHODS

Chemicals and solutions

Experimental solution compositions are shown in Table 1. All reagents, unless otherwise noted, were analytical grade. Nucleotides were obtained from Sigma Chemical Company (St. Louis, MO). Caged ATP and caged ADP were synthesized as in Walker et al. (1989) and contained less than 0.04% and 0.02%, respectively, residual contaminants as determined by reverse-phase HPLC. ADP was purified to greater than 99.9% by ion-exchange chromatography as described by Dantzig et al. (1991). The pure 5- and 6-isomers of IATR (see Fig. 1) were synthesized and characterized as previously described (Corrie and Craik, 1994). Bundles of rabbit psoas muscle fibers were dissected, skinned with glycerol, and stored as in Goldman et al. (1984a).

Fiber preparation and labeling

Muscle fibers were labeled with the 5- or 6-isomer of IATR as described by Tanner et al. (1992) and are referred to as being ATR labeled because the iodide atom of IATR is lost during the covalent modification of sulfhydryl sidechains. Briefly, fiber bundles were washed for 30 min in labeling buffer (LB: 80 mM KCl, 5 mM $MgCl_2$, 2 mM EGTA, 5 mM sodium phosphate buffer, 5 mM ATP, pH 7.0, 4°C), treated for 20 min with LB + 0.1% Triton X-100, washed again for 20 min with LB, reacted with 222 μM of either 5-IATR or 6-IATR in LB for 60 min, and then washed extensively with LB for 2–4 h before being returned to glycerol storage solution. All steps were carried out at 4°C in the dark. The extent of labeling at SH1 was determined from the fractional inhibition of the myosin K^+/EDTA ATPase activity (600 mM KCl, 50 mM MOPS, 5 mM Na_2ATP, 10 mM EDTA, pH 7.5, 25°C):

$$\text{fraction SH1 modified} = 1 - (A_{ATR}/A_{UL}),$$

where A_{ATR} and A_{UL} are the K^+/EDTA ATPase activities of myofibrils obtained from ATR-labeled and unlabeled muscle fiber bundles, respectively (Reisler, 1982; Crowder and Cooke, 1984). The rate of phosphate liberation was measured by the method of Lanzetta et al. (1979). We assessed further modification at SH2 (Cys-697 of the myosin heavy chain) by measuring the fractional change in the K^+/Ca^{2+} ATPase activity (600 mM KCl, 50 mM MOPS, 5 mM Na_2ATP, 10 mM $CaCl_2$, pH 7.5, 25°C) of the ATR-labeled myofibrils relative to unlabeled myofibrils (Reisler, 1982; Crowder and Cooke, 1984). Active and relaxed ATPase activities of ATR-labeled and unlabeled myofibrils were determined under conditions identical to those used in the muscle fiber experiments, but ATP was not added to the solutions until the start of the assay.

TABLE 1 Composition of experimental solutions

Solution	$MgCl_2$	Na_2ATP	Na_2ADP	Na_2CP	EGTA	CaEGTA	HDTA
Relaxing	7.7	5.4	0	19.1	25	0	0
0.1 mM MgATP relaxing	2.7	0.1	0	21.5	30	0	0
Rigor	3.2	0	0	0	52.7	0	0
Calcium rigor	1.3	0	0	0	0	20	32.6
Rigor with MgADP	4.1	0	2.0	0	20	0	26
Calcium rigor with MgADP	3.2	0	2.0	0	0	20	26
Preactivating	6.9	5.0	0	19.5	0.1	0	24.9
Activating	6.8	5.0	0	19.5	0	25.0	0

All concentrations are in mM. All solutions contained 100 mM TES (*N*-tris(hydroxymethyl)methyl-2-aminoethanesulfonic acid), 10 mM reduced glutathione, and 1 mM free Mg^{2+}. Relaxing solutions also contained 1 mg/ml creatine phosphokinase (≈100–200 units/mg activity). Solutions were made up at room temperature (20°C) and brought to a pH of 7.1 with KOH or HCl. The ionic strength of all solutions was 200 mM, and the major cations were Na^+ and K^+. Solutions with no added calcium contained $<10^{-8}$ M free Ca^{2+}, and solutions with added calcium contained ≈30 μM free Ca^{2+}. For photolysis solutions, concentrated rigor stock solutions, caged ATP or caged ADP, and H_2O were combined to yield the above concentrations plus 10 mM caged nucleotide. No adjustment was made for the ionic strength contribution of caged nucleotide. CP, creatine phosphate; EGTA, ethyleneglycol-bis-(β-aminoethylether)-*N,N,N',N'*-tetraacetic acid; HDTA, 1,6-diaminohexane-*N,N,N',N'*-tetraacetic acid.

We estimated labeling specificity of the myosin heavy chain by quantitating the fluorescence from SDS-polyacrylamide gels (5–15% linear gradient) of myofibrils obtained from ATR-labeled fiber bundles. We used Polaroid 667 black-and-white film to photograph gels for Rhodamine fluorescence under UV light. The photographs were digitized and quantitated on a Discovery Series desktop scanner (PDI, Huntington Station, NY) interfaced with PDI Quantity One analysis software (v. 2.4). Optical resolution was set at 64 μm in the reflectance mode, and the detector sensitivity was set to a linear range. We determined exposure times by calibrating the optical response of the Polaroid film with known amounts of 5-ATR-labeled bovine serum albumin. Following photography, gels were stained with Coomassie Brilliant Blue dye, and bands identified by comparison with protein standards of known molecular weight were run in adjacent lanes.

Fluorescent images of myofibrils obtained from ATR-labeled muscle fibers were recorded with a cooled CCD camera (CH220; Photometrics, Tucson, AZ) by Dr. Vladimir Zhukarevand Dr. Henry Shuman, using a Nikon Diaphot inverted microscope equipped with a Zeiss PlanApo 100 × 1.3-N.A. oil immersion phase contrast objective, a Rhodamine excitation and emission filter cube (Omega, Brattleboro, VT), and a 100-WHMO illuminator. Images were stored and processed as in Zhukarevetal. (1995).

Experimental apparatus

The apparatus for mechanical measurements on single, skinned muscle fibers following photolysis of caged nucleotides or rapid length changes was similar to that described previously by Goldman et al. (1984a). Single muscle fibers were dissected from bundles stored in glycerol, and short segments (2–3 mm) were cut and placed in aluminum T-clips. The muscle fiber segment was mounted by means of the T-clips to hooks on a strain-gauge force transducer (Sensonor, Norway; natural frequency ≈5 kHz) at one end and a moving coil motor (Cecchi et al., 1976) programmed for length steps at the other end. Length steps, complete within 200 μs, were applied either as a staircase of releases in which the muscle fiber was successively shortened by a fixed amount at 50-ms intervals or as a series of stretches and releases (equal in amplitude but separated by ≈5 ms) that were applied to the muscle fiber at 25-ms intervals. The fiber was bathed in different experimental solutions that were contained in one of five interchangeable stainless-steel troughs. Caged nucleotides were photolyzed with a frequency-doubled ruby laser (347 nm) focused on the fiber through a fused-silica window on the front of the first solution trough. We varied the amount of caged nucleotide photolyzed to release ATP or ADP in some experiments by placing one to eight glass slides between the frequency-doubled ruby laser and the muscle fiber. Sarcomere lengths and fiber dimensions were determined as described by Goldman and Simmons (1984).

Fluorescence polarization data were acquired essentially as described by Tanner et al. (1992) and Allen et al. (1996). Probes in ATR-labeled muscle fibers were excited through a fused-silica window in the bottom of the first solution trough by a continuous, 514-nm argon laser (model 5500A; ILT, Salt Lake City, UT; 100 mW attenuated to ≈1 mW at the muscle fiber). The polarization of the exciting light was alternated between orientations parallel ($\parallel$) and perpendicular ($\perp$) to the muscle fiber axis at a rate of 84.2 kHz by a photoelastic modulator (PEM-80 model FSA; Hinds International, Portland, OR). The emitted fluorescence, collected from above the muscle fiber, was separated into parallel and perpendicular components with respect to the muscle fiber axis by a Wollaston prism, and each signal ($\parallel$ and $\perp$) was collected by an independent photomultiplier tube (model R928; Hamamatsu, Bridgewater, NJ). The amplitudes ($D_\parallel$ and $D_\perp$) of the 84.2-kHz modulation of fluorescence intensity were extracted by two lock-in amplifiers (model 3961B; Ithaco, Ithaca, NY). The output of the two photomultiplier tubes was also passed through two 1-kHz low-pass filters (model 3100F; Pacific Instruments, Concord, CA) to yield the average fluorescence intensities ($L_\parallel$ and $L_\perp$) of the fluorescence signals. Tension, motor position, and the four optical signals ($D_\parallel$, $D_\perp$, $L_\parallel$, and $L_\perp$) were simultaneously sampled, digitized at 12-bit resolution and 500-μs sampling rate, and stored on disk by an 80386-based computer. Fluorescence polarization ratios (defined below) were calculated off-line from the digitized optical signals after the small background signal levels obtained with the exciting light blocked were subtracted and with scaling factors obtained with a random, immobilized sample of IATR as described by Allen et al. (1996).

Analysis of fluorescence polarization and mechanical transient data

Fluorescence polarization ratios, described in detail by Allen et al. (1996), were defined as

$$Q_\parallel = D_\parallel/L_\parallel = ({}_\parallel I_\parallel - {}_\perp I_\parallel)/({}_\parallel I_\parallel + {}_\perp I_\parallel),$$

$$Q_\perp = D_\perp/L_\perp = ({}_\perp I_\perp - {}_\parallel I_\perp)/({}_\perp I_\perp + {}_\parallel I_\perp),$$

where D and L are as defined above, I is the fluorescence intensity, and the left and right subscripts denote the polarization of the excitation and emission polarizers, respectively. The fluorescence polarization ratios can be used in a model-independent manner to assess qualitatively the orientational distribution of Rhodamine probes with respect to the muscle fiber axis as follows: If $Q_\perp < Q_\parallel$, then the average angle of the probes with respect to the muscle fiber axis is less than the magic angle (54.7°); if $Q_\perp > Q_\parallel$, then the average angle of the probes with respect to the muscle fiber axis is greater than 54.7°; if $Q_\parallel = Q_\perp$, then the probes are either oriented at 54.7° with respect to the muscle fiber axis or isotropically disordered.

To assess more quantitatively changes in the orientation of the Rhodamine labels, we fitted simple models of the probe orientational distributions to our data, using routines developed with Mathcad 6.0$^+$ software (Math Soft, Inc., Cambridge, MA). In all models the fluorophores are assumed to wobble within a cone of semiangle δ on a time scale that is fast compared with the fluorescent lifetime (Allen et al., 1996; Ling et al., 1996). The simplest model that fits the data assumes two populations of probes, one helically ordered at an angle Θ with respect to the axis of the muscle fiber and another population that is completely disordered (isotropic). This "helical plus isotropic" model requires that three parameters be fitted: Θ, f (the fraction of probes in the disordered group), and δ. We found that the data could be fitted only over a very limited range of values for δ and thus set δ = 0.2 rad (11.5°). Assuming this value of δ reduced the number of parameters to be fitted to two (Θ and f). In this model changes in the degree of disorder of the probe distribution among various physiological states are described as changes in f. A second, "Gaussian plus isotropic," model was also fitted to the data. In this model the probes were again assumed to have two populations, one completely disordered and one with a peak angle (Θ_0) and a Gaussian dispersion of σ about that angle ($n[\alpha] = \exp(-(1/2)((\alpha - \Theta_0)/\sigma)^2 \sin\alpha$; Allen et al., 1996). f was assumed to arise primarily from nonspecifically bound labels and was therefore set, along with δ, as a constant. f was varied from 0.3 to 0.6 based on the estimates of nonspecifically bound probes from SDS-PAGE experiments described below (see Table 2 in Results). For the 5-ATR- and 6-ATR-labeled fibers we found only one value of f (0.44) that produced exact fits for all the data when the other adjustable parameters were varied. If was f increased or decreased by even 0.01, exact fits for all the data were not obtained. The 6-ATR data could also be fitted with values of f in the range 0.44–0.55, presumably because of the slightly larger number of nonspecifically bound probes, but this resulted in no significant change in the fitted values of Θ_0 and in less than a 10% decrease in σ. Thus, for the sake of simplicity, we assumed values of f = 0.44 and δ = 11.5° for the data from both isomers, again reducing the number of parameters to be fitted to two (Θ_0 and σ). In this model changes in the extent of disorder of the probe distribution between physiological states are described as changes in the dispersion (σ) about the peak angle (Θ_0).

To compare the rate of cross-bridge detachment with the rate of change in the optical signals arising from Rhodamine probes at SH1, we fitted a simple three-state kinetic model to the tension transients generated by photolysis of caged ATP, using a nonlinear least-squares analysis (Fletcher

and Powell, 1963) implemented by Mr. Marcus Bell of our laboratory. This model (Scheme IV from Dantzig et al., 1991) included the rate of ATP photoliberation from caged ATP (118 s^{-1} at 20°C), detachment of rigor cross-bridges on ATP binding (k_D), and finally cross-bridge reattachment and force generation (k_A):

$$\text{Caged ATP} \xrightarrow{118\ s^{-1}} \text{ATP}$$
$$\text{rigor} \xrightarrow[k_D]{} \text{detached} \xrightarrow[k_A]{} \text{active.}$$

Reciprocal half-times (s^{-1}) for cross-bridge detachment were calculated from the fitted kinetic parameters of the model and compared with the reciprocal half-times measured from the fluorescence polarization transients. We estimated apparent second-order rate constants ($M^{-1}\ s^{-1}$) for cross-bridge detachment and changes in $Q_{\parallel}$ and $Q_{\perp}$ by minimizing the squared residuals between measured and predicted reciprocal half-times over a range of nucleotide concentrations, using a routine developed with Mathcad 6.0+. Myosin head concentration within the muscle fiber was assumed to be 150 μM (Ferenczi et al., 1984).

Experimental protocol

Single muscle fibers began each experiment in relaxing solution. For rigor experiments the fiber was sequentially moved from relaxing solution to 0.1 mM MgATP relaxing solution to rigor solution. Fibers were then transferred directly from rigor solution into rigor solution containing Ca^{2+}, ADP, caged ADP, or caged ATP. Fibers activated without caged ATP were transferred from relaxing solution into two washes of preactivating solution (0.1 mM EGTA, Table 1) and finally into an activating solution containing 5 mM MgATP and saturating Ca^{2+}. The fiber was incubated in each solution (except activating solution) for at least 2 min. Fluorescence polarization data were collected from the solution trough fitted with optical windows, and the fiber was returned directly to relaxing solution following each experimental trial. The amounts of ATP or ADP liberated by photolysis of caged ATP or caged ADP, respectively, were determined by HPLC analysis as previously described (Goldman et al., 1984a; Dantzig et al., 1991).

RESULTS

Labeling of fibers

The extent and specificity of labeling SH1 was examined by biochemical characterization of myofibrils obtained from muscle fibers labeled with either the 5- or the 6-isomer of IATR. These results are summarized in Table 2. Fractional inhibition of the K^+/EDTA ATPase activity of labeled myofibrils relative to that of unlabeled myofibrils was used as a measure of the extent of labeling at SH1 (Kielley and Bradley, 1956; Reisler, 1982; Crowder and Cooke, 1984). With either isomer, more than 50% of the myosin heads were labeled, but the extent of labeling at SH1 (Cys-707 of the myosin heavy chain) was greater with 5-ATR (71%) than with 6-ATR (57%). The K^+/Ca^{2+} ATPase activity of myosin is activated by labeling at SH1 but is inhibited if SH2 (Cys-697 of the myosin heavy chain) is also modified (Reisler, 1982; Crowder and Cooke, 1984). Myofibrils obtained from fibers labeled with either isomer of IATR had elevated K^+/Ca^{2+} ATPase activities relative to the unlabeled myofibrils. The K^+/Ca^{2+} activity was higher in the 5-ATR- than in the 6-ATR-labeled myofibrils, partly because the extent of labeling at SH1 was greater in the 5-ATR fibers. Moreover, the increase relative to unlabeled fibers in the K^+/Ca^{2+} ATPase activity of the 6-ATR-labeled fibers was less than that of the 5-ATR-labeled fibers. This result suggests that 6-IATR may be labeling more of SH2 than is 5-IATR, assuming that the increase of the K^+/Ca^{2+} ATPase activity that is due to labeling at SH1 is linearly related to the decrease in K^+/EDTA ATPase activity.

We estimated the specificity of each isomer for labeling the myosin heavy chain by quantifying the fluorescence from myofibrillar extracts run on SDS-polyacrylamide gels (Fig. 2). There were three major protein bands labeled in myofibrils reacted with either isomer of IATR: myosin, tropomyosin, and light chain 1, as determined by comparison with known molecular weight standards stained with Coomassie Blue. A small amount (<10%) of free-Rhodamine dye was also observed at the front of the gel only in those lanes containing extracts obtained from the 6-ATR-labeled fibers. Quantification of the fluorescence from the gels indicates that >50% of the total fluorescence was localized to the myosin heavy chain in fibers labeled with either 5-ATR (68%) or 6-ATR (53%). Fluorescence micrographs of myofibrils obtained from 5-ATR-labeled fibers

TABLE 2 Characterization of ATR-labeled fibers

	Unlabeled	5-ATR Labeled	6-ATR Labeled
Extent and specificity of labeling labeling			
K^+/EDTA ATPase activity*	0.732 ± 0.023	0.213 ± 0.016	0.315 ± 0.055
K^+/Ca^{2+} ATPase activity*	0.078 ± 0.004	0.180 ± 0.010	0.119 ± 0.005
Fraction SH1 modified	—	0.71 ± 0.02	0.57 ± 0.09
Labeling specificity	—	0.68 ± 0.02	0.53 ± 0.03
Physiological properties			
Relaxed ATPase activity*	0.012 ± 0.001	0.026 ± 0.001	0.023 ± 0.001
Active ATPase activity*	0.233 ± 0.009	0.186 ± 0.008	0.209 ± 0.006
Active tension (kN/m^2)	202 ± 17 (n = 9)	137 ± 18 (n = 19)	152 ± 23 (n = 14)

*All ATPase activity values are expressed in units of μmol phosphate (P_i) released per min per mg protein and are given as the mean ± SE for three sets of fiber bundles from separate animals. The fractional modification of SH1 and specificity of labeling the myosin heavy chain with 5-ATR or 6-ATR were determined on the same three sets of fiber bundles as described in Materials and Methods. The fraction of SH1 residues modified was determined from the fractional inhibition of the K^+/EDTA ATPase activity. Labeling specificity was determined from fluorescent images of myofibrillar extracts in SDS-polyacrylamide gels as in Fig. 2. Active tension values were obtained from single isometric muscle fibers and are given as the mean ± SE.

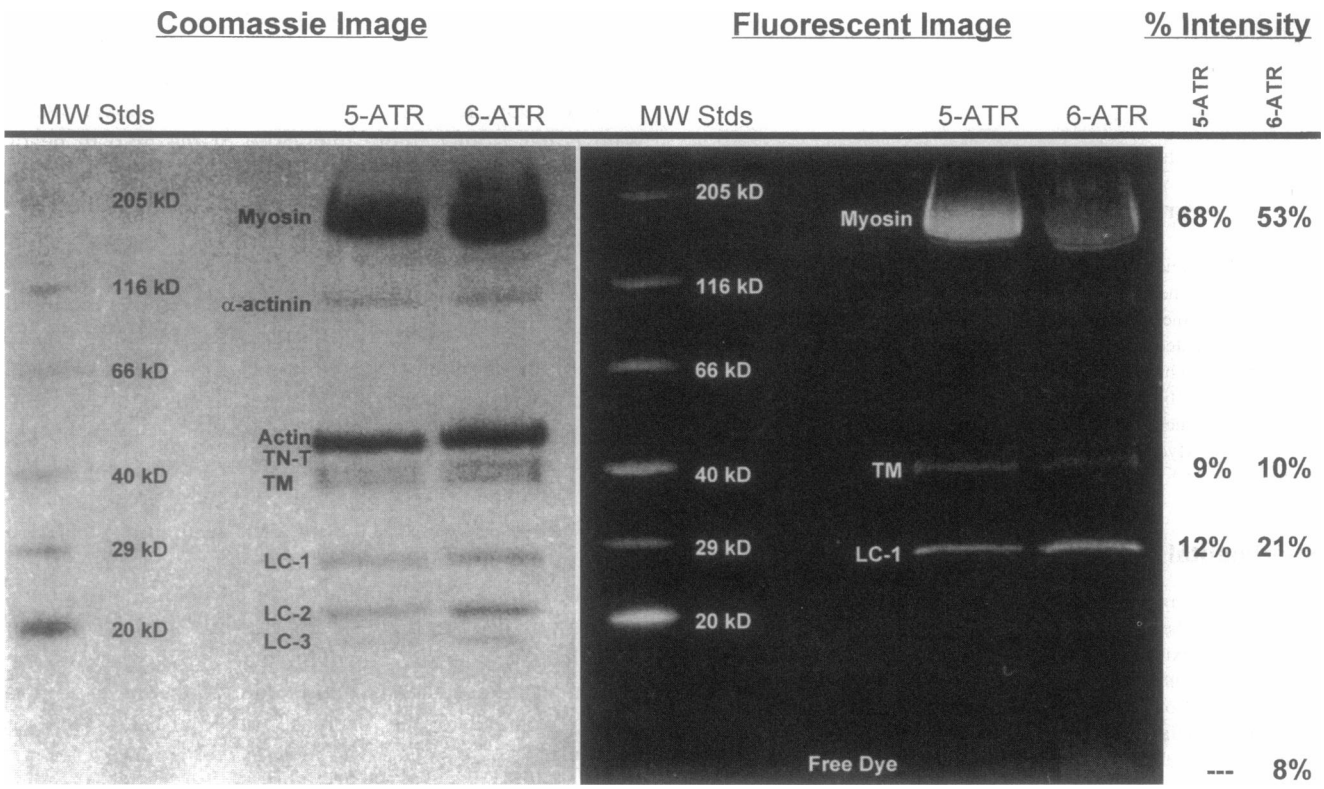

FIGURE 2 Coomassie Blue–stained and fluorescent images of a SDS-PAGE gel of myofibrils obtained from 5-ATR- and 6-ATR-labeled muscle fibers. Proteins were identified by their calculated molecular weights relative to known molecular weight standards. Relative intensities of the major fluorescent bands (*far right*) were determined by scanning densitometry of the fluorescent image of the SDS-PAGE gel obtained under UV illumination (see Materials and Methods). TN-T, troponin T; TM, tropomyosin; LC, myosin light chain.

show the fluorescence to be localized within the myosin-containing A band of the sarcomere (Fig. 3 *A*). Myofibrils obtained from the 6-ATR-labeled muscle fibers show a similar labeling pattern within the sarcomere, although additional labeling at the Z lines and in the H zone can also be observed (Fig. 3 *B*).

Modification of SH1 with either isomer of ATR resulted in limited changes in the basic physiological properties of the muscle fibers (Table 2). The relaxed ATPase activities of 5-ATR- and 6-ATR-labeled fibers were slightly elevated, and the calcium-activated ATPase activities of 5-ATR- and 6-ATR-labeled fibers were slightly depressed relative to those of unlabeled fibers. Active tension of 5-ATR- and 6-ATR-labeled muscle fibers was also depressed relative to that of unlabeled fibers. However, the relative levels of force reduction (25–35%) were less than the relative levels of SH1 modification (55–70%) for both the 5-ATR- and the 6-ATR-labeled muscle fibers (Table 2).

Steady-state fluorescence polarization

Steady-state values of fluorescence polarization for muscle fibers labeled with 5-ATR and 6-ATR are given in Table 3. The results are qualitatively similar for both isomers under all conditions studied. In rigor $Q_\perp$ is much greater than $Q_\parallel$, indicating that the average angle of the probes is more perpendicular than the magic angle (54.7°; Tregear and Mendelson, 1975; Irving, 1996) to the fiber axis. Addition of saturating Ca^{2+} to rigor fibers slightly increases the difference between $Q_\parallel$ and $Q_\perp$, indicating a more ordered overall probe distribution. Addition of caged ATP and caged ADP to rigor, on the other hand, decrease the difference between $Q_\parallel$ and $Q_\perp$, which is indicative of a slightly more disordered overall probe distribution. In actively contracting or ADP-rigor fibers $Q_\parallel$ is greater than $Q_\perp$, indicating a substantial reorientation of the Rhodamine probes with the addition of nucleotide and a more axial distribution of probe orientation than in rigor. Furthermore, the values of $Q_\parallel$ and $Q_\perp$ are also closer together in the presence of nucleotide than in rigor, indicating a more disordered overall probe distribution. The addition of 10 mM phosphate to active fibers depressed force by approximately 30% (data not shown) but produced only a very slight change in the fluorescence polarization ratios. In relaxed fibers $Q_\parallel$ and $Q_\perp$ are almost equal, indicating a highly disordered population of probes.

Fluorescence polarization following photolysis of caged nucleotides

To examine the temporal relationship between force generation and the reorientation of Rhodamine probes at SH1

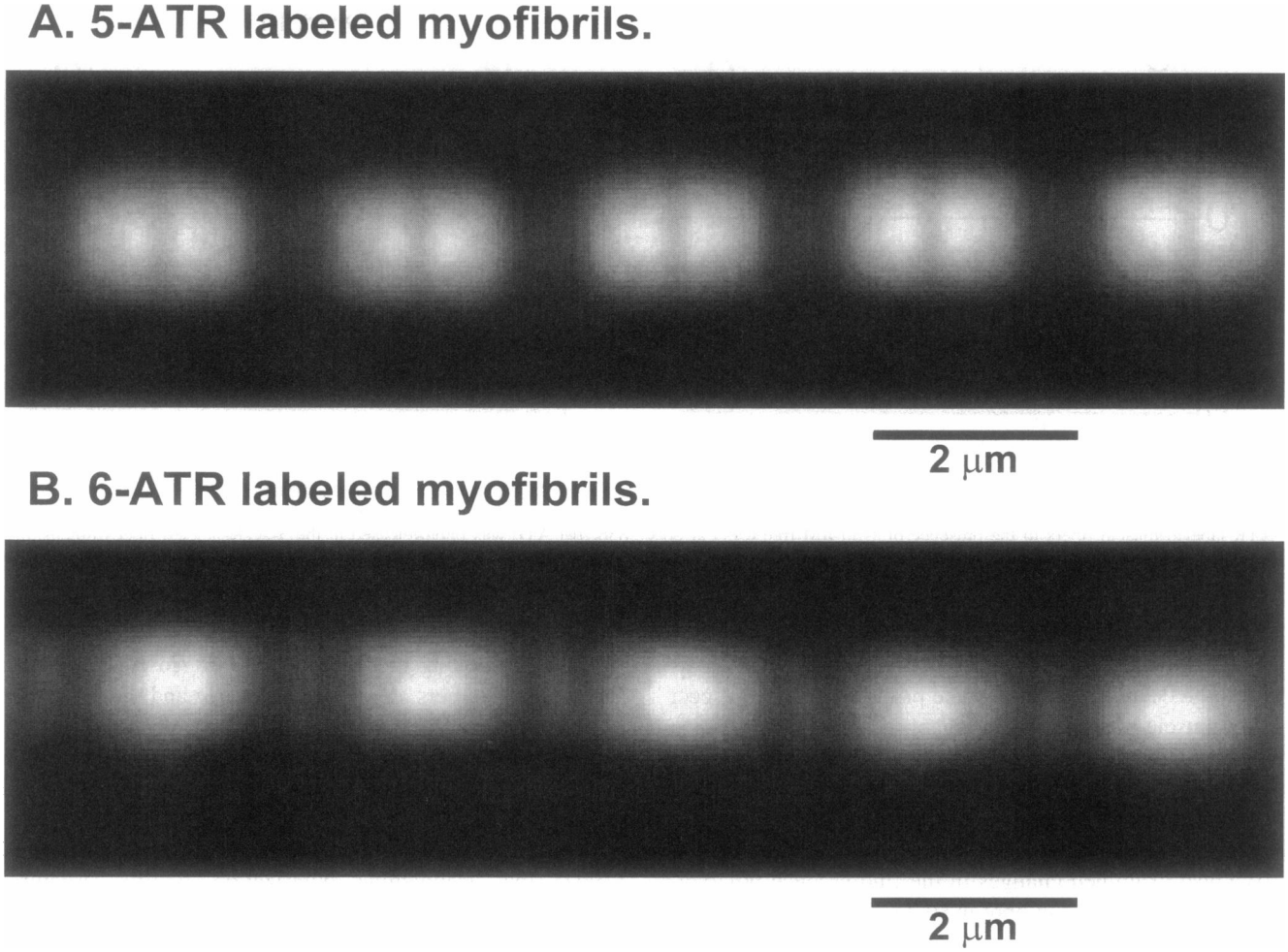

FIGURE 3 Fluorescent images of myofibrils obtained from 5-ATR- and 6-ATR-labeled muscle fibers. Each image contains five consecutive sarcomeres from a single myofibril.

during activation of muscle fibers from rigor, we simultaneously recorded force transients and fluorescence polarization ratios on photolysis of caged ATP in the presence of saturating Ca^{2+}. In Fig. 4 the muscle fibers are in rigor (no nucleotide) before photolysis, and for both the 5-ATR- and the 6-ATR-labeled fibers $Q_\perp$ is greater than $Q_\parallel$, indicating that the probes are preferentially oriented perpendicular to the muscle fiber axis. In both 5-ATR- and 6-ATR-labeled fibers, photolysis of caged ATP induces large and very rapid changes in the fluorescence polarization ratios, as expected from the steady-state data. $Q_\parallel$ increases and $Q_\perp$ decreases, causing the two polarization ratio signals to cross following

TABLE 3 Steady-state fluorescence polarization ratios

	5-ATR Fibers			6-ATR Fibers		
Solution	$Q_\parallel$	$Q_\perp$		$Q_\parallel$	$Q_\perp$	
Relaxing	0.442 ± 0.004	0.416 ± 0.003	(n = 12)	0.450 ± 0.005	0.371 ± 0.003	(n = 11)
Activating	0.467 ± 0.006	0.372 ± 0.003	(n = 19)	0.435 ± 0.002	0.396 ± 0.002	(n = 14)
Active + 10 mM P_i	0.443 ± 0.002	0.383 ± 0.005	(n = 3)	0.436 ± 0.002	0.392 ± 0.003	(n = 3)
Rigor	0.310 ± 0.008	0.633 ± 0.008	(n = 11)	0.341 ± 0.006	0.518 ± 0.007	(n = 11)
Ca^{2+} rigor	0.268 ± 0.008	0.660 ± 0.007	(n = 12)	0.314 ± 0.006	0.537 ± 0.007	(n = 10)
Rigor + ADP	0.498 ± 0.010	0.393 ± 0.007	(n = 5)	0.466 ± 0.002	0.390 ± 0.004	(n = 5)
Ca^{2+} rigor + ADP	0.480 ± 0.010	0.433 ± 0.007	(n = 5)	0.442 ± 0.004	0.412 ± 0.003	(n = 4)
Ca^{2+} rigor + cATP	0.402 ± 0.002	0.624 ± 0.004	(n = 30)	0.382 ± 0.004	0.506 ± 0.005	(n = 19)
Ca^{2+} rigor + cADP	0.419 ± 0.010	0.579 ± 0.004	(n = 6)	0.373 ± 0.020	0.535 ± 0.015	(n = 5)

Solutions are as defined in Table 1; cATP, caged ATP; cADP, caged ADP. $Q_\parallel$ and $Q_\perp$ were calculated as defined in Materials and Methods. Values given are the mean ± SE.

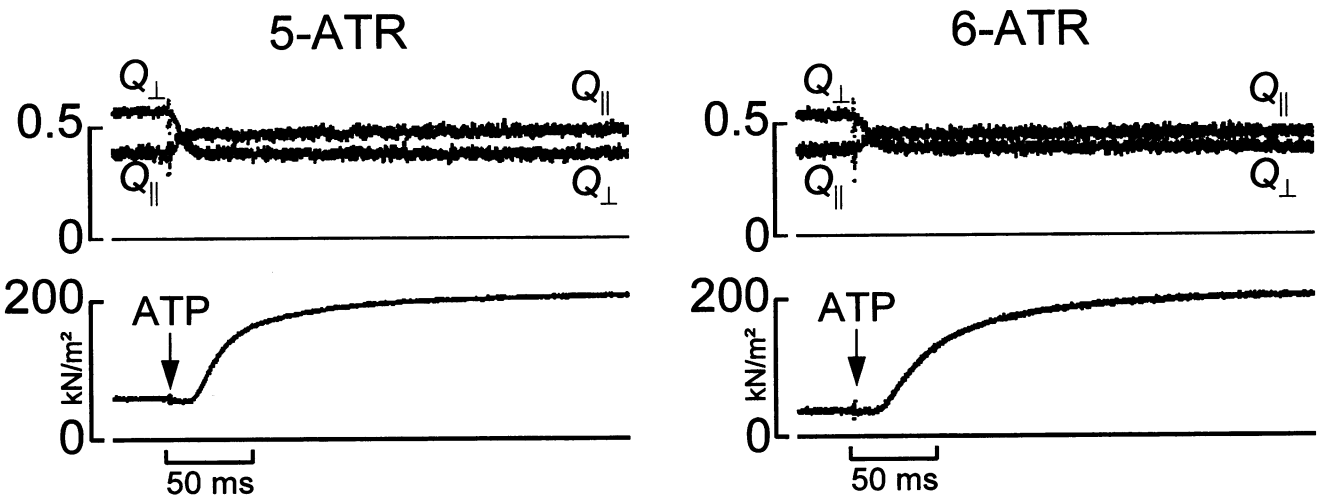

FIGURE 4 Fluorescence polarization (*top*) and force (*bottom*) transients elicited by photorelease of ATP from caged ATP (*arrows*) in 5-ATR- and 6-ATR-labeled muscle fibers in the presence of ≈30 μM free Ca^{2+} at 20°C. 836 μM ATP was photoreleased in the 5-ATR-labeled fiber (dimensions: sarcomere length, 2.43 μm; fiber length, 2.33 mm; cross-sectional area, 5447 μm^2). 699 μM ATP was photoreleased in the 6-ATR-labeled fiber (dimensions: sarcomere length, 2.52 μm; fiber length, 2.88 mm; cross-sectional area, 5423 μm^2).

photorelease of ATP. $Q_\parallel$ becomes greater than $Q_\perp$, indicating a large decrease in the average probe angle with respect to the muscle fiber axis. The changes in the fluorescence polarization signals are virtually complete well before the muscle fiber develops appreciable active tension, suggesting that the structural changes that occur at SH1 on activation are not concomitant with force generation.

We also examined changes in the fluorescence polarization ratios following the photolysis of caged ADP (Fig. 5). In contrast to ATP, ADP causes only a small decrease in force when it binds to myosin in the muscle fiber and therefore does not induce a power stroke. However, on photolysis of caged ADP the time course and the magnitude of the changes in $Q_\parallel$ and $Q_\perp$ are very similar to those observed following the photolysis of caged ATP for both Rhodamine isomers, despite the opposite and much smaller change in force. The two fluorescence polarization traces again cross following the photorelease of ADP, indicating a significant redistribution of the probe orientations toward the fiber axis, as expected from the steady-state results. These kinetic results support the conclusion of Tanner et al. (1992) that Rhodamine polarization reports structural changes at SH1 that are more closely related to nucleotide binding than to the force-generating step of the contractile cycle.

Inasmuch as on photolysis of caged ATP the fluorescence polarization ratios change substantially before the main force development, we considered whether the structural

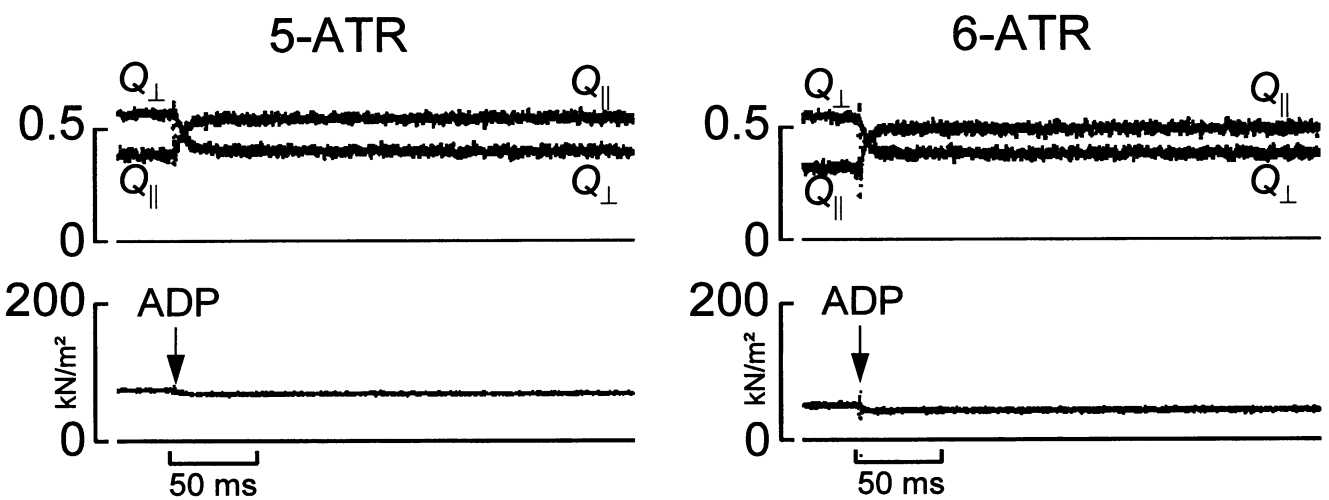

FIGURE 5 Fluorescence polarization (*top*) and force (*bottom*) transients elicited by photorelease of ADP from caged ADP (*arrows*) in 5-ATR- and 6-ATR-labeled muscle fibers at 20°C. 819 μM ADP was photoreleased in the 5-ATR-labeled fiber (dimensions: sarcomere length, 2.43 μm; fiber length, 2.33 mm; cross-sectional area, 5447 μm^2). 851 μM ADP was photoreleased in the 6-ATR-labeled fiber (dimensions: sarcomere length, 2.52 μm; fiber length, 2.88 mm; cross-sectional area, 5423 μm^2).

changes relate to the initial detachment of rigor cross-bridges by ATP binding. Over a range of photoreleased ATP concentrations, we estimated the apparent rate of cross-bridge detachment following photolysis of caged ATP by fitting a simple kinetic model (Scheme IV, Dantzig et al., 1991) to the resulting tension transients (Fig. 6). Reciprocal half-times for cross-bridge detachment were calculated from these fits and compared with the reciprocal half-times measured from the fluorescence polarization transients. The dependence of the observed reciprocal half-times for the changes of $Q_{\parallel}$, $Q_{\perp}$, and cross-bridge detachment on [ATP] are shown in Fig. 7 for fibers labeled with both isomers of ATR. For the 5-ATR-labeled fibers, $Q_{\parallel}$ changes slightly faster than $Q_{\perp}$ following photolysis of caged ATP, and both polarization signals generally change faster than does the apparent rate of cross-bridge detachment. Apparent second-order rate constants for cross-bridge detachment ($0.67 \times 10^5\ M^{-1}\ s^{-1}$) and changes in $Q_{\parallel}$ ($1.35 \times 10^5\ M^{-1}\ s^{-1}$) and $Q_{\perp}$ ($1.12 \times 10^5\ M^{-1}\ s^{-1}$) were determined for each data set as described in Materials and Methods. Because the myosin active sites are not fully saturated at low ATP concentrations, the dependence of reciprocal half-times for cross-bridge detachment and changes in $Q_{\parallel}$ and $Q_{\perp}$ on nucleotide concentration rises more steeply at low [ATP] than would be predicted by a single apparent second-order rate constant. Comparable results are observed with the 6-ATR-labeled fibers, and apparent second-order rate constants were also calculated for cross-bridge detachment ($0.97 \times 10^5\ M^{-1}\ s^{-1}$) and changes in $Q_{\parallel}$ ($1.38 \times 10^5\ M^{-1}\ s^{-1}$) and $Q_{\perp}$ ($1.14 \times 10^5\ M^{-1}\ s^{-1}$).

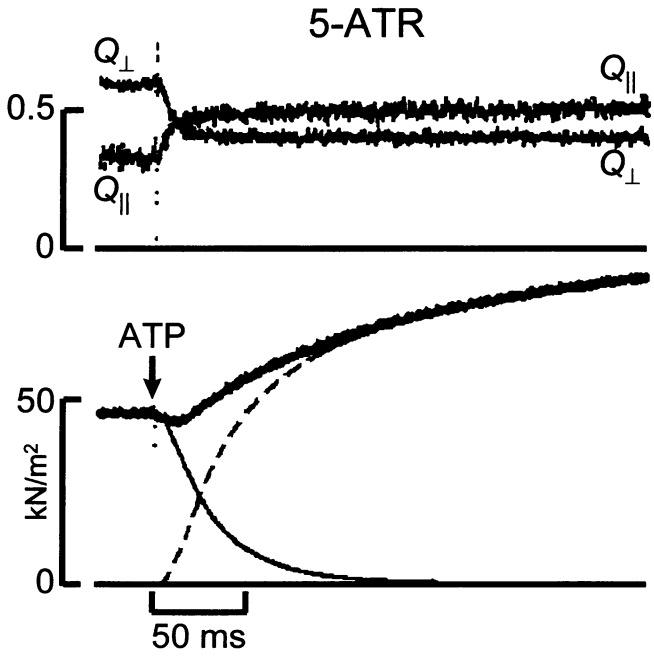

FIGURE 6 Fit of a simple kinetic model (see Materials and Methods) to tension transients elicited by photorelease of 676 μM ATP from caged ATP (*arrow*) in a 5-ATR labeled muscle fiber in the presence of $\approx$30 μM free Ca^{2+} at 20°C. Superimposed upon the tension transient are the estimated rates of cross-bridge detachment (*solid curve*) and active force generation by cross-bridge reattachment (*dashed curve*). Fluorescence polarization transients (*top*) are shown for comparison. Fiber dimensions: sarcomere length, 2.38 μm; fiber length, 2.32 mm; cross-sectional area, 5019 μm^2.

The rates of change of $Q_{\parallel}$ and $Q_{\perp}$ following photolysis of caged ADP are slightly faster than those observed following the photolysis of caged ATP. For the 5-ATR-labeled fibers the apparent second-order rate constants observed are $2.10 \times 10^5\ M^{-1}\ s^{-1}$ for $Q_{\parallel}$ and $2.01 \times 10^5\ M^{-1}\ s^{-1}$ for $Q_{\perp}$ (data not shown). Although we did not measure the rates of change of $Q_{\parallel}$ and $Q_{\perp}$ following photorelease of a range of ADP concentrations in the 6-ATR-labeled fibers, it is evident from Fig. 5 that they are approximately the same for both the 5-ATR- and the 6-ATR-labeled fibers.

Fluorescence polarization following rapid length steps

Another method for synchronizing events in the cross-bridge cycle is to apply rapid length changes to the muscle fiber (A.F. Huxley and Simmons, 1971). For releases, there is an initial drop in tension concomitant with the length step, followed by a partial recovery of force as the cross-bridges undergo partly synchronized power strokes. We examined changes in fluorescence polarization following rapid length steps in active and rigor muscle fibers (Fig. 8). To ensure that possible small changes in $Q_{\parallel}$ or $Q_{\perp}$ would be detected, we averaged multiple tension and fluorescence polarization traces for both the active and the rigor experiments (Irving et al., 1995). Each trace consisted of a staircase or repeated sequence of identical length changes that were averaged together as well, resulting in an $\approx$6-fold total improvement of signal-to-noise ratio over that for single events. However, even for large releases (12 nm/half-sarcomere) of 5-ATR-labeled muscle fibers during active contraction there is no significant change in the fluorescence polarization ratios during the step or the quick recovery of force. The same is true for stretches and releases up to 10 nm/half-sarcomere in 5-ATR-labeled muscle fibers in rigor, in which all the cross-bridges are presumably attached to actin. These results suggest that the myosin domain containing SH1 does not rotate relative to actin either during an active contraction or in rigor.

DISCUSSION

Modification of Cys-707 by IATR

We used fluorescence polarization to examine orientational changes of Rhodamine probes in single muscle fibers following either photolysis of caged nucleotides or rapid length changes. Fibers were preferentially labeled at SH1 (Cys-707) of the myosin heavy chain with either the 5- or the 6-isomer of IATR, although the extent and the specificity of SH1 labeling were found to be slightly greater for the 5-isomer (Table 2). The extent of modification at SH1 with each isomer was greater than previously reported (0.37) by

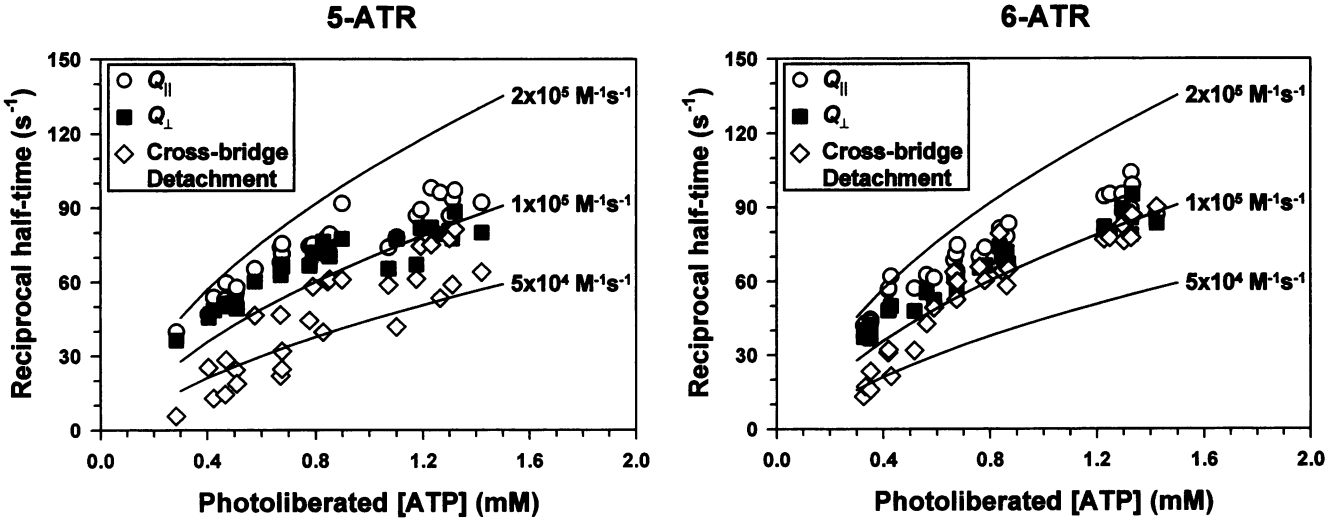

FIGURE 7 Dependence of the reciprocal half-times for cross-bridge detachment and changes in $Q_{\parallel}$ and $Q_{\perp}$ on the concentration of photoliberated ATP for 5-ATR- and 6-ATR-labeled muscle fibers in the presence of ≈30 μM free Ca^{2+} at 20°C. The solid curves show the predicted reciprocal half-times as a function of ATP concentration calculated for the apparent second-order rate constant shown to the right of each curve and include the rate of photoliberation of ATP from caged ATP (118 s^{-1} at 20°C).

Tanner et al. (1992). The significant increase in SH1 modification is most likely due to the purity of the probes used in the present study (Corrie and Craik, 1994), which do not contain the unidentified contaminants found in the commercial preparations of mixed isomers used by Tanner et al. (1992). Ajtai et al. (1992) reported that 6-IATR labels primarily actin, not myosin, in conflict with the present results. The lack of reactivity of the 6-IATR probes with SH1 in the research of Ajtai et al. (1992) may have been caused by contaminants in the commercial preparation of IATR that effectively competed with the probe for SH1 or blocked its reaction at that site. We observed little evidence of noncovalently bound Rhodamine probes in our preparations. Free-Rhodamine dye was not detectable in lanes of our SDS-polyacrylamide gels containing extracts from the 5-ATR-labeled muscle fibers, and less than 10% of the Rhodamine was observed as free dye in lanes containing extracts from the 6-ATR-labeled muscle fibers. Thus the present results indicate that most or all of the changes in the fluorescence polarization signals reported here and in Tanner et al. (1992) during flash photolysis and rapid length changes arise from Rhodamine probes at SH1 of the myosin heavy chain.

It is important to consider the effect of extensive SH1 modification on the physiological properties of the muscle fiber. Root and Reisler (1991) have suggested that SH1

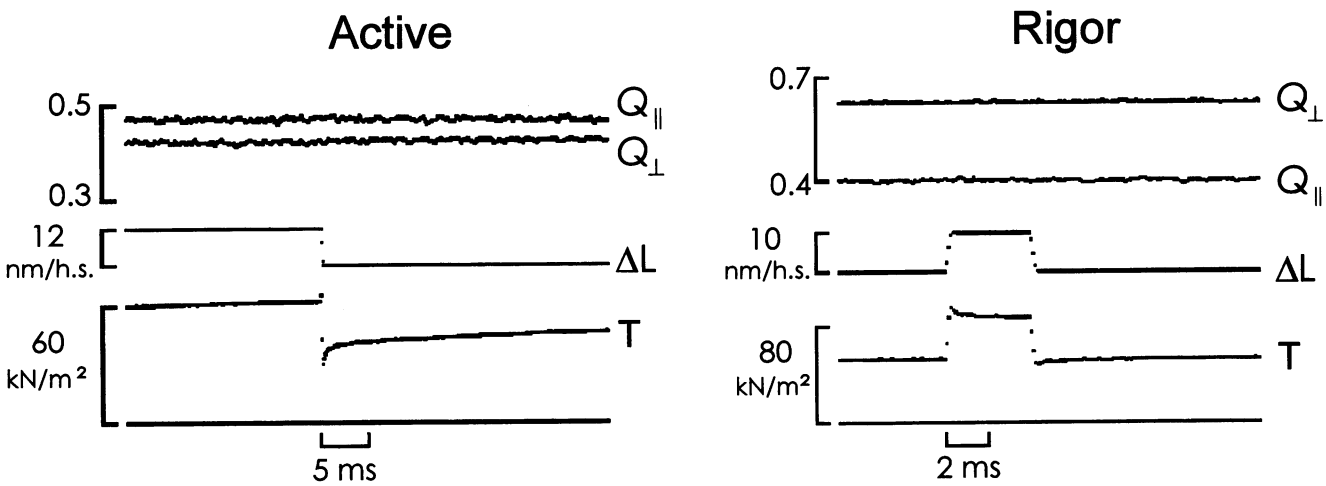

FIGURE 8 Fluorescence polarization ($Q_{\parallel}$ and $Q_{\perp}$) and force (T) transients elicited by rapid length changes (ΔL) in active and rigor 5-ATR-labeled muscle fibers. The data shown are the average response of the fiber to a total of 32 length steps over 4 active (5 mM MgATP and ≈30 μM free Ca^{2+}) or 2 rigor (no added ATP or Ca^{2+}) contractions at 20°C. Length steps (complete within 200 μs) were applied as a staircase of releases during active contractions and as a series of stretches and releases in rigor. Fiber dimensions: initial sarcomere length, 2.45 μm; fiber length, 2.16 mm; cross-sectional area, 5853 μm^2.

modified cross-bridges are not active but can enhance that catalytic activity of unmodified myosin heads, resulting in a nonlinear relationship between force production and degree of sulfhydryl modification in myosin. However, other studies have demonstrated that modification of SH1 does not inactivate myosin but alters the kinetics of the cross-bridge cycle by slowing the rate of ATP hydrolysis, shifting the population of strongly bound cross-bridges toward the weakly bound states, and reducing the number of strongly bound cross-bridges during an isometric contraction (Sleep et al., 1981; Matta and Thomas, 1992; Bell et al., 1995; Raucher et al., 1995). The net result of this modification is an approximately 70% reduction in isometric force and steady-state ATP hydrolysis in fibers almost completely modified at SH1. We observed similar, but smaller, effects on ATPase activity and isometric force in our labeled muscle fibers. The difference between the present results and those of previous studies (Matta and Thomas, 1992; Bell et al., 1995) is probably due to the lower fraction of modified SH1 groups in our preparation. For both 5-ATR and 6-ATR fibers the relative decrease in force was appreciably less than the level of SH1 modification, suggesting that SH1-labeled myosin heads generate force, albeit less than unmodified heads. The estimated rate of cross-bridge detachment in the Rhodamine-labeled muscle fibers is also somewhat slower than that of unlabeled muscle fibers ($5 \times 10^5\ M^{-1}\ s^{-1}$; Goldman et al., 1984a,b), which is likely to be related to the slower kinetics of SH1-modified cross-bridges (Sleep et al., 1981). Thus, it appears that SH1-labeled cross-bridges can actively hydrolyze ATP and generate force, and therefore the major features described here concerning Rhodamine-labeled cross-bridges are applicable to unmodified cross-bridges as well.

Steady-state fluorescence polarization

Polarization ratios (Q signals) were qualitatively similar for the 5-ATR- and the 6-ATR-labeled muscle fibers. However, under many conditions the difference between $Q_\parallel$ and $Q_\perp$ was smaller in muscle fibers labeled with 6-ATR than in those labeled with 5-ATR. These results suggest a more disordered probe distribution in the 6-ATR-labeled fibers than in the 5-ATR-labeled fibers, probably because of the greater number of nonspecifically attached 6-ATR probes. The fact that both preparations are highly disordered in the presence of nucleotide indicates that the nonspecific probes are nearly randomly distributed. The similarity in the fluorescence polarization data from fibers labeled with either of the isomers suggests that both probes report the same structural changes at SH1. This conclusion again conflicts with the report of Ajtai et al. (1992) that only 5-ATR is sensitive to the physiological state of the muscle fiber. The difference between the two studies is most likely due to the difference in purity of the probes used and the consequent effect on labeling reactivity and specificity as discussed above.

In the presence of nucleotide (e.g., ADP-rigor, relaxation, activation), the static fluorescence polarization ratios of 5-ATR- and 6-ATR-labeled muscle fibers were quite similar. Under all these conditions $Q_\parallel$ was only slightly greater than $Q_\perp$, suggesting that the Rhodamine probe distribution is disordered, with an average angle of slightly less than the magic angle (54.7°). In rigor, the difference between the polarization ratios is greatly increased, with $Q_\perp$ becoming greater than $Q_\parallel$, suggesting a more ordered probe population than in the presence of nucleotide. Furthermore, the average angle of the probes also increases in rigor to greater than 54.7°. The small but consistent change in the polarization ratios on addition of calcium to fibers in rigor indicates a slight tilt of the probes away from the fiber axis. This tilt may be due to an effect of calcium either on the cross-bridges or on another protein that was also labeled. Distinguishing between these possibilities will require further experiments. The addition of caged ATP or caged ADP to rigor fibers decreases the difference between $Q_\parallel$ and $Q_\perp$, indicating a slight disordering of the probes. This is probably so because caged ATP and caged ADP bind weakly to myosin with affinity in the millimolar range (Thirlwell et al., 1995), and thus a small population of the cross-bridges is likely to be in the nucleotide bound state that disorders the Rhodamine probes at SH1.

It was previously shown by use of linear dichroism measurements that a substantial change in the orientational distribution of the probes at SH1 follows the addition of MgADP or MgATP (Borejdo et al., 1982; Burghardt et al., 1983; Tanner et al., 1992) to Rhodamine-labeled muscle fibers in rigor. In all those studies the average probe angle with respect to the fiber axis was greater than the magic angle (54.7°) in rigor and less than the magic angle in the presence of nucleotide. Although the numerical value of the calculated probe angle is model dependent, the changed sign of the dichroism in the previous studies (Borejdo et al., 1982; Burghardt et al., 1983; Tanner et al., 1992) and the switch between $Q_\perp > Q_\parallel$ in rigor to $Q_\parallel > Q_\perp$ in the presence of nucleotide (Table 3 and Figs. 4–6 of this paper) indicate that a net rotation of the probe population toward the fiber axis follows addition of nucleotide, independently of models of the orientational distribution of the probes.

To relate the polarization values quantitatively to changes in the orientational distribution of the probes we fitted two different models, "helical plus isotropic" and "Gaussian plus isotropic" (as described in Materials and Methods), to the data (Table 4). It should be noted that the actual orientational distribution of the Rhodamine probes is probably much more complex than can be described by models that contain only the few adjustable parameters that can be constrained by our data. In rigor both models produce similar values for the average angle of the ordered population of probes (Θ, Θ_0) in fibers labeled with either the 5- or the 6-isomer of IATR. A larger fraction of probes appears to be disordered in rigor fibers labeled with 6-ATR (0.67) than in the rigor fiber labeled with 5-ATR (0.52), in agreement with the larger estimate of nonspecifically bound probes for the 6-ATR isomer (see Table 2). However, the dispersion of probes about Θ_0 in the Gaussian plus isotropic model (σ) is

TABLE 4 Orientational distribution parameters

	Helical plus isotropic model			
	5-ATR Fibers		6-ATR Fibers	
	θ (°)	f	θ (°)	f
Relaxing	47.3	0.88	43.2	0.81
Activating	40.9	0.82	46.8	0.84
Rigor	73.3	0.52	66.8	0.67
Ca^{2+} rigor	73.7	0.45	67.7	0.62
Rigor + ADP	36.1	0.86	41.2	0.85
Ca^{2+} rigor + ADP	38.3	0.93	46.9	0.87
	Gaussian plus isotropic model			
	5-ATR Fibers		6-ATR Fibers	
	θ_0 (°)	σ (°)	θ_0 (°)	σ (°)
Relaxing	46.4	24.7	44.4	21.7
Activating	41.9	23.5	46.8	22.1
Rigor	79.0	21.1	62.3	20.1
Ca^{2+} rigor	73.9	5.1	64.8	17.7
Rigor + ADP	33.8	30.9	42.1	25.2
Ca^{2+} rigor + ADP	36.5	34.9	46.3	24.3

The helical plus isotropic and the Gaussian plus isotropic models are as defined in Materials and Methods. δ was set equal to 11.5° for both models. f was set equal to 0.44 for the Gaussian plus isotropic model.

almost identical for 5-ATR- and 6-ATR-labeled rigor fibers. Addition of calcium in the rigor solution has only very small effects on Θ or Θ_0 and slightly decreases f and σ for fibers labeled with either isomer. The addition of ATP or ADP to a rigor fiber, in either the absence or the presence of calcium, induces a major change in the orientational distribution of both isomers of ATR. In the helical plus isotropic model the helically ordered probes become more axial in the presence of nucleotide, and the fraction of disordered probes increases substantially.

Under all conditions studied, the peak angles of the Gaussian distribution (Θ_0) determined for the ordered population of probes in the Gaussian plus isotropic model are not much different from the angles (Θ) calculated for the helically ordered probes in the helical plus isotropic model. However, addition of ATP or ADP to rigor fibers results only in modest increases of the dispersion (σ) about Θ_0 for fibers labeled with either isomer. This limited range of values for σ is surprising considering the large increase in f on the addition of nucleotide to rigor fibers in the helical plus isotropic model. Both models support the existence of a significant population of well-ordered Rhodamine probes in rigor, with a substantial axial reordering of the probes on nucleotide binding, for both the 5-ATR- and the 6-ATR-labeled fibers. This is consistent with the qualitative, model-independent, analysis of the Q signals given in Results. However, in the presence of nucleotide the helix plus random model is consistent with the majority of Rhodamine probes' becoming isotropically disordered, whereas the random plus Gaussian model predicts a significant population of ordered probes with only a relatively small increase ($\leq$20°) in the dispersion about their mean angle. The fact that $Q_\parallel$ and $Q_\perp$ have similar values does indeed suggest a more disordered distribution of the Rhodamine probes at SH1 in the presence of nucleotide for fibers labeled with either isomer, but the estimated amount of disordering is quite model dependent. In the actual distribution there are probably more than two distinct populations of probes, and a complete description of the structural changes at SH1 will require additional information to refine potential models further.

Fluorescence polarization transients

Despite the very different tension transients elicited by photorelease of ADP and ATP, transients of the Q signals after photolysis have similar time courses and amplitudes. Following activation by photolysis of caged ATP, force decreases and then increases substantially; whereas, following photolysis of caged ADP, force rapidly decreases by a small amount. On photolysis of caged ATP the fluorescence polarization transients are much faster than force development and may even precede cross-bridge detachment, as estimated by kinetic analysis. No changes in the Q signals were observed following even large-amplitude, rapid length steps in active and rigor muscle fibers, indicating no change in the orientational distribution of the probes at SH1. These results support the conclusion of Tanner et al. (1992) that structural changes at SH1 detected by Rhodamine probes are not directly related to the myosin power stroke during force generation.

Allen et al. (1996), using regulatory light chains (LC-2 or RLC) labeled mainly with 6-ATR from a commercial preparation, also observed fast transients of fluorescence polarization that accompany either ATP binding or the subse

quent cross-bridge dissociation. In that study, as in the present experiments, the Q traces were virtually flat during the onset of tension development following activation by photolysis of caged ATP. Irving et al. (1995) found, in contrast to the present data, that in muscle fibers labeled on the RLC with pure 6-ATR, quick length changes elicit transients of fluorescence polarization both during the length change and during the quick recovery within the subsequent few milliseconds. Possible explanations of why Rhodamine probes on the RLC are sensitive to structural changes during force development following rapid length changes but not following photolysis of caged ATP are discussed in detail by Allen et al. (1996). The simplest explanation for the difference in response to length changes in RLC- versus SH1-labeled fibers is that the light chain–binding region of the myosin head tilts during length changes and the subsequent quick recovery, whereas the nucleotide- and actin-binding region of myosin containing SH1 does not. Although it is possible that the probes at SH1 are positioned at an unfavorable orientation to detect angle changes induced by mechanical strain, the change in average orientation between rigor and active contraction make it unlikely that the probe disposition would be unfavorable in both states.

Solution of the crystal structure of myosin subfragment-1 (S1) has shown the head to be composed of a catalytic domain containing the nucleotide- and actin-binding sites and an extended C-terminal α-helix that binds both the essential and the regulatory light chains (Rayment et al., 1993b). An important revision of the conventional rotating cross-bridge model suggested from the crystal structure is that the myosin head does not rotate as a rigid unit but rather that the catalytic domain that contains SH1 remains rigidly bound to actin while the C-terminal α-helix and light chains tilt as a mechanical lever arm (Rayment et al., 1993a). In support of the role of the light chain region as a lever arm, VanBuren et al. (1994), using an in-vitro motility assay, found that the amount of force generated by a cross-bridge depends on the number of light chains bound to myosin and thus apparently on the length of the lever arm. The finding of Irving et al. (1995) that Rhodamine probes on the RLC change orientation in response to rapid length changes suggests that tilting of the light chain–binding region has a direct role in force production. Our results are also consistent with this model of force generation. The lack of change in the orientational distribution of probes at SH1 suggests that the catalytic domain does not rotate during the power stroke.

ADP release and the power stroke

The substantial change in linear dichroism of Rhodamine probes at SH1 when ADP binds to the rigor cross-bridge was taken by Borejdo et al. (1982) and Burghardt et al. (1983) as evidence for a concerted angular change of the probes related to the myosin power stroke. The present results, and our earlier dichroism experiments (Tanner et al., 1992), are consistent with this change in dichroism, but many other studies indicating small or negligible structural and mechanical changes on ADP binding to rigor muscle appear to rule out the linkage between ADP release and the power stroke (Rodger and Tregear, 1974; Fajer et al., 1990a; Dantzig et al., 1991; Obiorah and Irving, 1989; Takemori et al., 1995; Allen et al., 1996). Recent helical reconstructions based on electron micrographs of actin filaments decorated with myosin subfragment-1 have shown large changes in the angle of the light chain–binding region when ADP binds (Whittaker et al., 1995; Jontes et al., 1995). However, the myosin molecules used in those studies had sequences derived from smooth muscle and brush border myosin. It was recently shown by EPR spectroscopy that, unlike in smooth muscle myosin, the light chain–binding region of skeletal muscle myosin does not rotate on ADP binding (Gollub et al., 1996). The weight of evidence suggests that the probe angle changes observed here on nucleotide binding to attached cross-bridges report a localized structural change rather than a global motion of the head.

Role of structural changes at SH1 in muscle contraction

The switch from rigor to active contraction results in a net axial shift of the probe orientational distribution and a considerable apparent disordering. Other studies utilizing EPR and time-resolved phosphorescence anisotropy to examine the orientation and mobility of probes at SH1 in muscle fibers have also found this region of myosin to be dynamically disordered during active, isometric contraction (Barnett and Thomas, 1989; Fajer et al., 1990b; Stein et al., 1992; Berger and Thomas, 1993). It has been suggested that the power stroke involves a disorder-to-order transition rather than the commonly assumed switch from one static angle to another (Berger and Thomas, 1994; Raucher and Fajer, 1994; Thomas et al., 1995). Our results are consistent with a model of muscle contraction in which the SH1 region of myosin is largely disordered during the power stroke. The techniques used here do not detect a transition to an ordered population of probes during force generation. This observation may indicate that during contraction the ordered population of probes at SH1 is too small to contribute to the fluorescence intensity, that the Rhodamine probes are more sensitive to the local conformation around SH1 than the spin labels used in EPR experiments, or that the SH1 region of myosin does not rotate in a concerted manner during the power stroke and remains disordered throughout force development. These possibilities are not mutually exclusive, and the negligible change in fluorescence polarization following rapid length changes in active and rigor muscle fibers, despite large changes in force in both cases, suggests the two last-named possibilities.

What is the role of the structural changes that are observed at SH1 in the molecular mechanism of contraction?

Cross-linking studies have demonstrated the movement of SH1 and SH2 (Cys697) some 10 Å toward each other on nucleotide binding to myosin (Wells and Yount, 1979; Huston et al., 1988). SH1 has been shown to be located on a short α-helix that lies near both the nucleotide-binding pocket and the base of the large cleft that separates the two portions of the 50-kD domain of chicken skeletal muscle subfragment-1 (Rayment et al., 1993b). Addition of nucleotide analogs results in significant structural changes around SH1 in the crystal structure of a truncated subfragment-1 from the slime mold *Dictyostelium discoideum* (Fisher et al., 1995; Smith and Rayment, 1995; 1996). The cleft that splits the 50-kD domain is partially closed, the orientation of the α-helix containing SH1 is rotated by 20° and translated 2.5 Å relative to the nucleotide-free subfragment-1 crystal structure, and the electron density becomes quite disordered just beyond SH1 (Fisher et al., 1995; Smith and Rayment, 1996). These results are consistent with the probe disorder at SH1 in our fluorescence polarization experiments, although the fact that the subfragment-1 construct is truncated just past SH1 in the crystals may also account for some of the observed disorder. However, together these results suggest a large conformational change in subfragment-1 on nucleotide binding that may involve a melting or breaking of the helices containing SH1 and SH2 (Rayment et al., 1993a).

It has been suggested that the large cleft that divides the 50-kD domain of subfragment-1 plays a critical role in mediating the strength of the interaction between actin and myosin (Rayment et al., 1993a). Our results are consistent with this hypothesis. The structural changes detected by the fluorescence polarization signals occur very rapidly following the photolysis of caged nucleotides. Not only do these structural changes at SH1 precede force generation but they even appear slightly earlier than cross-bridge detachment. Thus the observed deflection of the polarization signals on nucleotide binding may relate to the weakening of myosin's affinity for actin. Structural changes at the active site induced by nucleotide binding may propagate through SH1 to residues near the large cleft that divides the 50-kD domain and finally to the actin-binding region of myosin. Thus the structural changes at SH1 are not synchronous with the force-generating event of muscle contraction but may be involved in the communication pathway between the nucleotide- and actin-binding sites of myosin.

We thank Dr. David D. Thomas and Dr. Malcolm Irving for their invaluable help and insight throughout this project, Dr. Vladimir Zhukarev and Dr. Henry Shuman for the fluorescent images of our labeled myofibrils, Mr. Joe Pili for his skilled mechanical design and construction, Dr. Michael Beers for his help with the densitometry of our gels, Dr. Jody Dantzig for providing us with purified ADP and caged compounds, Mr. Marcus Bell for software support, Mr. Gerry Hatcher for making solutions and HPLC analysis, and Mr. Sher Karki and Ms. Julia Schiffman for their effort during some of the experiments. This research was supported by National Institutes of Health grant AR26846 to Y.E.G., the UK Medical Research Council, and the Muscular Dystrophy Association of America.

REFERENCES

Ajtai, K., P. J. K. Ilich, A. Ringler, S. S. Sedarous, D. J. Toft, and T. P. Burghardt. 1992. Stereospecific reaction of muscle fiber proteins with the 5′ or 6′ isomer of (iodoacetamido)tetramethylrhodamine. *Biochemistry.* 31:12,431–12,440.

Allen, T. St. C., N. Ling, M. Irving, and Y. E. Goldman. 1996. Orientation changes in myosin regulatory light chains following photorelease of ATP in skinned muscle fibers. *Biophys. J.* 70:1847–1862.

Barnett, V. A., and D. D. Thomas. 1989. Microsecond rotational motion of spin-labeled myosin heads during isometric muscle contraction. *Biophys. J.* 56:517–523.

Bell, M. G., J. J. Matta, D. D. Thomas, and Y. E. Goldman. 1995. Changes in cross-bridge kinetics induced by SH-1 modification in rabbit psoas fibers. *Biophys. J.* 68:360s.

Berger, C. L., J. S. Craik, D. R. Trentham, J. E. T. Corrie, and Y. E. Goldman. 1994a. Fluorescence polarization of acetamidotetramethylrhodamine (ATR) isomers covalently bound to SH-1 in rabbit psoas muscle fibers following activation by photolysis of caged ATP. *Biophys. J.* 66:234a.

Berger, C. L., J. S. Craik, D. R. Trentham, J. E. T. Corrie, and Y. E. Goldman. 1995a. Fluorescence polarization changes and mechanical events following photolysis of caged ATP in rabbit psoas muscle fibers labeled at SH-1 with isomers of acetamidotetramethylrhodamine (ATR). *Biophys. J.* 68:10a.

Berger, C. L., J. S. Craik, D. R. Trentham, J. E. T. Corrie, and Y. E. Goldman. 1995b. Fluorescence polarization from isomers of tetramethylrhodamine at SH-1 in rabbit psoas muscle fibers. *Biophys. J.* 68: 78s–80s.

Berger, C. L., S. Karki, and Y. E. Goldman. 1994b. Fluorescence polarization of acetamidotetramethylrhodamine (ATR) bound to SH-1 in rabbit psoas muscle fibers following rapid length changes. *Biophys. J.* 66:189a.

Berger, C. L., E. C. Svensson, and D. D. Thomas. 1989. Photolysis of a photolabile precursor of ATP (caged ATP) induces microsecond rotational motions of myosin heads bound to actin. *Proc. Natl. Acad. Sci. USA.* 86:8753–8757.

Berger, C. L., and D. D. Thomas. 1993. Rotational dynamics of actin-bound myosin heads in active myofibrils. *Biochemistry.* 32:3812–3821.

Berger, C. L., and D. D. Thomas. 1994. Rotational dynamics of actin-bound intermediates of the myosin adenosine triphosphatase cycle in myofibrils. *Biophys. J.* 67:250–261.

Borejdo, J., O. Assulin, T. Ando, and S. Putnam. 1982. Cross-bridge orientation in skeletal muscle measured by linear dichroism of an extrinsic chromophore. *J. Mol. Biol.* 158:391–414..

Burghardt, T. P., T. Ando, and J. Borejdo. 1983. Evidence for cross-bridge order in contraction of glycerinated skeletal muscle. *Proc. Natl. Acad. Sci. USA.* 80:7515–7519.

Cecchi, G., F. Colomo, and V. Lombardi. 1976. A loudspeaker servo system for determination of mechanical characteristics of isolated muscle fibres. *Boll. Soc. It. Biol. Speri.* LII:733–736.

Cooke, R., M. S. Crowder, and D. D. Thomas. 1982. Orientation of spin labels attached to cross-bridges in contracting muscle fibres. *Nature (London).* 300:776–778.

Corrie, J. E. T., and J. S. Craik. 1994. Synthesis and characterisation of pure isomers of iodoacetamidotetramethylrhodamine. *J. Chem. Soc. Perkin Trans. 1.* 2967–2973.

Crowder, M. S., and R. Cooke. 1984. The effect of myosin sulphydryl modification on the mechanics of fibre contraction. *J. Musc. Res. Cell Motil.* 5:131–146.

Dantzig, J. A., M. G. Hibberd, D. R. Trentham, and Y. E. Goldman. 1991. Cross-bridge kinetics in the presence of MgADP investigated by photolysis of caged ATP in rabbit psoas muscle fibres. *J. Physiol.* 432: 639–680.

Fajer, P. G., E. A. Fajer, J. J. Matta, and D. D. Thomas. 1990a. Effect of ADP on the orientation of spin-labeled myosin heads in muscle fibers: a high-resolution study with deuterated spin labels. *Biochem.* 29: 5865–5871.

Fajer, P. G., E. A. Fajer, and D. D. Thomas. 1990b. Myosin heads have a broad orientational distribution during isometric muscle contraction:

time-resolved EPR studies using caged ATP. *Proc. Natl . Acad. Sci. USA.* 87:5538–5542.

Ferenczi, M. A., E. Homsher, and D. R. Trentham. 1984. The kinetics of magnesium adenosine triphosphate cleavage in skinned muscle fibres of the rabbit. *J. Physiol.* 352:575–599.

Fisher, A. J., C. A. Smith, J. B. Thoden, R. Smith, K. Sutoh, H. M. Holden, and I. Rayment. 1995. X-ray structures of the myosin motor domain of *Dictyostelium discoideum* complexed with MgADP·BeFx and MgADP·AlF_4^-. *Biochemistry.* 34:8960–8972.

Fletcher, R., and M. J. D. Powell. 1963. A rapidly convergent descent method for minimization. *Computer J.* 6:163–168.

Goldman, Y. E., M. G. Hibberd, and D. R. Trentham. 1984a. Relaxation of rabbit psoas muscle fibres from rigor by photochemical generation of adenosine-5′-triphosphate. *J. Physiol.* 354:577–604.

Goldman, Y. E., M. G. Hibberd, and D. R. Trentham. 1984b. Initiation of active contraction by photogeneration of adenosine-5′-triphosphate in rabbit psoas muscle fibres. *J. Physiol.* 354:605–624.

Goldman, Y. E., and R. M. Simmons. 1984. Control of sarcomere length in skinned muscle fibres of *Rana temporaria* during mechanical transients. *J. Physiol.* 350:497–518.

Gollub, J., C. R. Cremo, and R. Cooke. 1996. ADP release produces rotation of the neck region of smooth myosin but not skeletal myosin. *Nature Struct. Biol.* In press.

Huston, E. E., J. C. Grammer, and R. G. Yount. 1988. Flexibility of the myosin heavy chain: direct evidence that the region containing SH1 and SH2 can move 10 Å under the influence of nucleotide binding. *Biochemistry.* 27:8945–8952.

Huxley, A. F., and R. M. Simmons. 1971. Proposed mechanism of force generation in striated muscle. *Nature (London).* 233:533–538.

Huxley, H. E. 1969. The mechanism of muscular contraction. *Science.* 164:1356–1366.

Irving, M. 1996. Steady-state polarization from cylindrically symmetric fluorophores undergoing rapid restricted motion. *Biophys. J.* 70: 1830–1835.

Irving, M., T. StC. Allen, C. Sabido-David, J. S. Craik, B. Brandmeier, J. Kendrick-Jones, J. E. T. Corrie, D. R. Trentham, and Y. E. Goldman. 1995. Tilting of the light-chain region of myosin during step length changes and active force generation in skeletal muscle. *Nature (London).* 375:688–691.

Jontes, J. D., E. M. Wilson-Kubalek, and R. A. Milligan. 1995. A 32° tail swing in brush border myosin I on ADP release. *Nature (London).* 378:751–753.

Kaplan, J. H., B. Forbush, and J. Hoffman. 1978. Rapid photolytic release of adenosine-5′-triphosphate from a protected analogue: utilization by the Na:K pump of human red blood cell ghosts. *Biochemistry.* 17: 1929–1935.

Kielley, W. W., and L. B. Bradley. 1956. The relationship between sulfhydryl groups and the activation of myosin adenosinetriphosphatase. *J. Biol. Chem.* 218:653–659.

Lanzetta, P. A., L. J. Alvarez, P. S. Reinach, and O. A. Candia. 1979. An improved assay for nanomole amounts of inorganic phosphate. *Analyt. Biochem.* 100:95–97.

Ling, N., C. Shrimpton, J. Sleep, J. Kendrick-Jones, and M. Irving. 1996. Fluorescent probes of the orientation of myosin regulatory light chains in relaxed, rigor and contracting muscle. *Biophys. J.* 70:1836–1846.

Matta, J. J., and D. D. Thomas. 1992. Biochemical and mechanical effects of spin-labeling myosin SH1. *Biophys. J.* 61:295a.

Obiorah, O., and M. Irving. 1989. ADP binding to rigor crossbridges produces no major change in their conformation. *Biophys. J.* 55:9a.

Raucher, D., and P. G. Fajer. 1994. Orientation and dynamics of myosin heads in aluminum fluoride induced pre-power stroke states: an EPR study. *Biochemistry.* 33:11,993–11,999.

Raucher, D., E. A. Fajer, C. Sár, K. Hideg, Y. Zhao, M. Kawai, and P. G. Fajer. 1995. A novel electron paramagnetic resonance spin label and its application to study the cross-bridge cycle. *Biophys. J.* 68:128s–134s.

Rayment, I., H. M. Holden, M. Whittaker, C. B. Yohn, M. Lorenz, K. C. Holmes, and R. A. Milligan. 1993a. Structure of the actin-myosin complex and its implications for muscle contraction. *Science.* 261: 58–65.

Rayment, I., W. R. Rypniewski, K. Schmidt-Bäse, R. Smith, D. R. Tomchick, M. M. Benning, D. A. Winkelmann, G. Wesenberg, and H. M. Holden. 1993b. Three-dimensional structure of myosin subfragment-1: a molecular motor. *Science.* 261:50–58.

Reisler, E. 1982. Sulfhydryl modification and labeling of myosin. *Methods Enzymol.* 85:84–93.

Rodger, C. D., and R. T. Tregear. 1974. Crossbridge angle when ADP is bound to myosin. *J. Mol. Biol.* 86:495–497.

Root, D. D., and E. Reisler. 1991. Catalytic cooperativity induced by SH-1 labeling of myosin filaments. *Biochemistry.* 30:286–294.

Sleep, J. A., K. M. Trybus, K. A. Johnson, and E. W. Taylor. 1981. Kinetic studies of normal and modified heavy meromyosin and subfragment-1. *J. Musc. Res. Cell Motil.* 2:373–399.

Smith, C. A., and I. Rayment. 1995. X-ray structure of the magnesium(II)-pyrophosphate complex of the truncated head of *Dictyostelium discoideum* myosin to 2.7 Å resolution. *Biochemistry.* 34:8973–8981.

Smith, C. A., and I. Rayment. 1996. X-ray structure of the magnesium(II)·ADP·vanadate complex of the *Dictyostelium discoideum* myosin motor domain to 1.9 Å resolution. *Biochemistry.* 35:5404–5417.

Stein, R. A., R. D. Ludescher, P. S. Dahlberg, P. G. Fajer, R. L. H. Bennett, and D. D. Thomas. 1990. Time-resolved rotational dynamics of phosphorescent-labeled myosin heads in contracting muscle fibers. *Biochem. J.* 29:10,023–10,031.

Takemori, S., M. Yamaguchi, and N. Yagi. 1995. Effects of adenosine diphosphate on the structure of myosin cross-bridges: an x-ray diffraction study on a single skinned forg muscle fibre. *J. Musc. Res. Cell Motil.* 16:571–577.

Tanner, J. W., D. D. Thomas, and Y. E. Goldman. 1992. Transients in orientation of a fluorescent cross-bridge probe following photolysis of caged nucleotides in skeletal muscle fibres. *J. Mol. Biol.* 223:185–203.

Thirlwell, H., J. A. Sleep, and M. A. Ferenczi. 1995. Inhibition of unloaded shortening velocity in permeabilized muscle fibres by caged ATP compounds. *J. Musc. Res. Cell Motil.* 16:131–137.

Thomas, D. D., S. Ramachandran, O. Roopnarine, D. W. Hayden, and E. M. Ostap. 1995. The mechanism of force generation in myosin: a disorder-to-order transition, coupled to internal structural changes. *Biophys. J.* 68:135s–141s.

Tregear R. T., and R. A. Mendelson. 1975. Polarization from a helix of fluorophores and its relation to that obtained from muscle. *Biophys. J.* 15:455–467.

VanBuren, P., G. S. Waller, D. E. Harris, K. M. Trybus, D. M. Warshaw, and S. Lowey. 1994. The essential light chain is required for full force production by skeletal muscle myosin. *Proc. Natl. Acad. Sci. USA.* 91:12,403–12,407.

Walker, J. W., G. P. Reid, and D. R. Trentham. 1989. Synthesis and properties of caged nucleotides. *Methods Enzymol.* 158:288–301.

Wells, J. A., and R. G. Yount. 1979. Active site trapping of nucleotides by cross-linking two sulfhydryls in myosin. *Proc. Natl. Acad. Sci. USA.* 83:9433–9437.

Whittaker, M., E. M. Wilson-Kubalek, J. E. Smith, L. Faust, R. A. Milligan, and H. L. Sweeney. 1995. A 35-Å movement of smooth muscle myosin on ADP release. *Nature (London).* 378:748–753.

Zhukarev, V., F. Ashton, J. M. Sanger, J. W. Sanger, and H. Shuman. 1995. Organization and structure of actin filament bundles in *Listeria*-infected cells. *Cell Motil. Cytoskel.* 30:229–246.